

Rapid Communications

Rapid Communications are intended for the accelerated publication of important new results and are therefore given priority treatment both in the editorial office and in production. A Rapid Communication in Physical Review B should be no longer than four printed pages and must be accompanied by an abstract. Page proofs are sent to authors.

Electronic properties of the ordered delafossite-type superoxides $\text{YCuO}_{2+\delta}$

L. F. Mattheiss

AT&T Bell Laboratories, Murray Hill, New Jersey 07974

(Received 13 October 1993)

Electronic-structure calculations have been carried out on the ordered delafossite-type superoxides $\text{YCuO}_{2+\delta}$ ($0.5 \leq \delta \leq 0.7$) that Cava *et al.* have synthesized recently by inserting interstitial O into the triangular Cu planes of YCuO_2 . The results exhibit a unique feature where each interstitial O inserts two half-filled, cluster-derived Cu_3O_7 "impurity levels" into the ~ 2.7 -eV semiconductor gap of YCuO_2 . These levels evolve into half-filled "impurity bands" as adjacent clusters are corner-linked to form continuous one-dimensional (1D) linear ($\delta \approx \frac{1}{2}$) and 2D planar ($\delta \approx \frac{2}{3}$) networks that may exhibit interesting transport and magnetic properties.

The family of ABO_2 delafossite-type compounds has an ancestry which dates back to the discovery¹ of the mineral "delafossite" (i.e., FeCuO_2) in the late 1930s. These ternary oxides, which form with several hexagonal and rhombohedral ($2H$, $3R$, and $6H$) structural polytypes, represent a growing family of compounds that now includes about 30 members.²⁻⁶ The delafossite structure consists of four-layer O-A-O-B sequences in which the coordination of the trivalent A atom is octahedral whereas that of the monovalent B atom is linear. The different polytypes result from variations in the stacking and alignment of the O-A-O-B subunits. Recently, Cava *et al.*⁷ have succeeded in further oxidizing the ordinary delafossite-type compounds YCuO_2 and LaCuO_2 to form new ordered superoxides $\text{YCuO}_{2+\delta}$ and $\text{LaCuO}_{2+\delta}$ in which extra oxygen ($0.5 \leq \delta \leq 0.7$) is inserted interstitially into the triangular Cu planes. Structural studies⁷ show that at least two distinct O-ordered superlattices occur, including a monoclinic $M(\sqrt{3} \times 2)$ phase near $\delta = \frac{1}{2}$ and a hexagonal $H(\sqrt{3} \times \sqrt{3})$ superlattice near $\delta = \frac{2}{3}$.

These delafossite-derived superoxides represent an interesting analog to the cuprate high- T_c superconductors. Since the formal valence of Cu is $1+$ in undoped YCuO_2 and LaCuO_2 , the insertion of additional O into the structure is expected to increase the Cu valence to $2+$ and beyond for $\delta \geq \frac{1}{2}$. As a result, these systems provide opportunities to investigate the magnetic properties of triangular lattices of spin one-half Cu^{2+} ions where the "frustrated" nearest-neighbor antiferromagnetic interactions may lead to novel magnetic phenomena. These $\text{YCuO}_{2+\delta}$ and $\text{LaCuO}_{2+\delta}$ superoxides present both similarities and differences when compared with typical cuprate superconductor parent compounds such as

$\text{YBa}_2\text{Cu}_3\text{O}_6$, where the spin one-half Cu^{2+} ions are arranged on a square lattice and antiferromagnetic ordering is observed⁸ at 500 K. For example, the Y-Ba-Cu-O system contains both Cu^{1+} and Cu^{2+} sites, and oxygen doping suppresses rather than promotes antiferromagnetism, leading ultimately to metallic as well as superconducting behavior.

The purpose of the present study is to analyze the effects of oxygen doping on the basic electronic properties

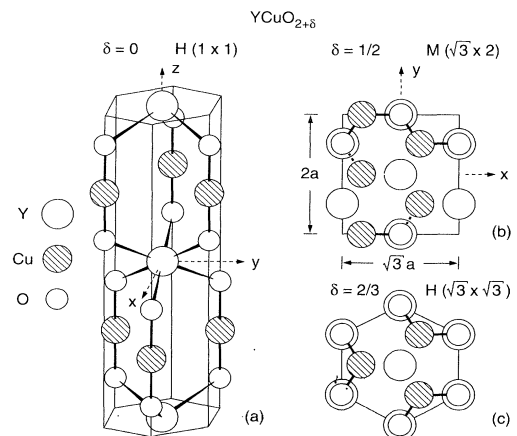


FIG. 1. (a) Primitive unit cell for the undoped hexagonal delafossite YCuO_2 . Basal-plane projection of atom positions for ordered superoxides $\text{YCuO}_{2+\delta}$, including the (b) $\delta = \frac{1}{2}$ monoclinic $M(\sqrt{3} \times 2)$, and (c) $\delta = \frac{2}{3}$ hexagonal $H(\sqrt{3} \times \sqrt{3})$ phases. The Y, Cu, and O (interstitial) atoms are at heights 0, $c/4$, and $c/2$, respectively. Dashed Cu-O bonds identify the threefold-coordinated Cu sites in the $M(\sqrt{3} \times 2)$ phase.

of YCuO_2 by tracing their evolution as extra O is added to form ordered $\text{YCuO}_{2+\delta}$ superoxides. Although this study has focused solely on $\text{YCuO}_{2+\delta}$, similar behavior is expected in $\text{LaCuO}_{2+\delta}$. This investigation has involved the combined use of the linear augmented-plane-wave⁹ (LAPW) and tight-binding (TB) methods. In the LAPW phase, the electronic band structure of the ordinary $2H\text{-YCuO}_2$ compound^{5,10} has been calculated along with that for a hypothetical YCuO_3 phase in which the partially occupied O sites of the $\text{YCuO}_{2+\delta}$ superoxides¹¹ are fully occupied. Using TB parameters derived from accurate fits (~ 0.18 eV rms error) to the YCuO_2 and YCuO_3 LAPW results, a TB scheme has been applied to calculate the band properties of O-ordered intermediate $\text{YCuO}_{2+\delta}$ phases where the basic YCuO_2 subunit has either quadrupled [i.e., $M(\sqrt{3}\times 2)\text{YCuO}_{2.5}$] or tripled [$H(\sqrt{3}\times\sqrt{3})\text{YCuO}_{2.67}$].

The essential features of the undoped $H(1\times 1)$ delafossite structure YCuO_2 are illustrated in Fig. 1(a). The Bravais lattice is hexagonal ($a = 3.52$ Å and $c = 11.42$ Å) and each primitive cell contains two formula units. The Y at the origin is octahedrally coordinated by six O's at distances ~ 2.27 Å while each Cu is linearly coordinated by two oxygen neighbors at ~ 1.83 Å to form O-Cu-O sticks. The Y, Cu, and O constituents are located at the (2a), (2c), and (4f) sites of the $P6_3/mmc$ (D_{6h}^4) space group.⁵ The observed¹¹ O-ordered superlattices are illustrated to the right. The interstitial O occupies sites at the centers of the Cu triangles in Fig. 1(a), producing a planar Cu-O bond length of ~ 2.03 Å which is $\sim 11\%$ larger

than that of the O-Cu-O sticks. Completely filling these planar interstitial sites produces the hypothetical YCuO_3 phase mentioned above while partial filling leads to the monoclinic $M(\sqrt{3}\times 2)$ superlattice for $\delta = \frac{1}{2}$ that is shown in Fig. 1(b) and the $\delta = \frac{2}{3}$ hexagonal $H(\sqrt{3}\times\sqrt{3})$ superstructure of Fig. 1(c). The present study has considered idealized superstructures in which atom positions are unrelaxed and inversion symmetry is assumed to maintain the same O-ordering patterns in neighboring Cu-O planes.

The present LAPW calculations for the $H(1\times 1)$ delafossite-type compounds YCuO_2 and YCuO_3 have been carried out self-consistently in the local-density approximation (LDA) using a full-potential implementation⁹ that imposes no shape approximations on either the charge density or the potential. Exchange and correlation effects have been included via the Wigner interpolation formula.¹² The LAPW basis has included plane waves with a 13.6-Ry cutoff (~ 350 LAPW's per formula unit) and spherical-harmonic terms through $l=8$ inside the muffin-tin spheres. The charge density and potential have been expanded using ~ 6500 plane waves in the interstitial region and lattice harmonics with $l_{\text{max}}=6$ within the muffin tins. Brillouin-zone integrations have utilized a 14-point \mathbf{k} sample. The calculations treat the $\text{Y}(4d^{15}s^2)$, $\text{Cu}(3d^{10}4s^1)$, and $\text{O}(2s^22p^4)$ atomic levels as valence states while a rigid-core approximation is applied to the remaining inner-shell electrons.

The LAPW results for YCuO_2 in the left panel of Fig. 2 show that this undoped phase is a large-gap (~ 2.7 eV) semiconductor in which the filled 22-band valence manifold evolves from nearly degenerate $\text{Cu}(3d)$ and $\text{O}(2p)$ levels while the lowest conduction bands are derived from

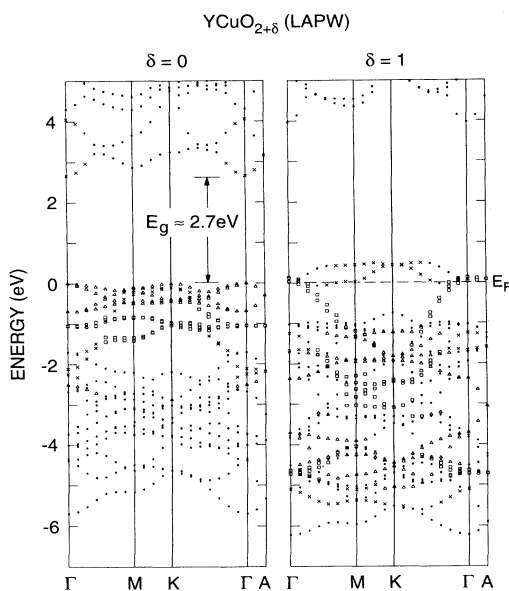


FIG. 2. LAPW energy-band results for YCuO_2 and (hypothetical) YCuO_3 along three basal-plane symmetry lines ($\Gamma\text{MK}\Gamma$) and one c -axis direction (ΓA) of the hexagonal Brillouin zone. Distinctive symbols identify bands containing at least 30% d_{xy} - $d_{x^2-y^2}$ (squares), d_{xz} - d_{yz} (triangles), or $d_{3z^2-r^2}$ (crosses) orbital weight inside the Cu muffin tins.

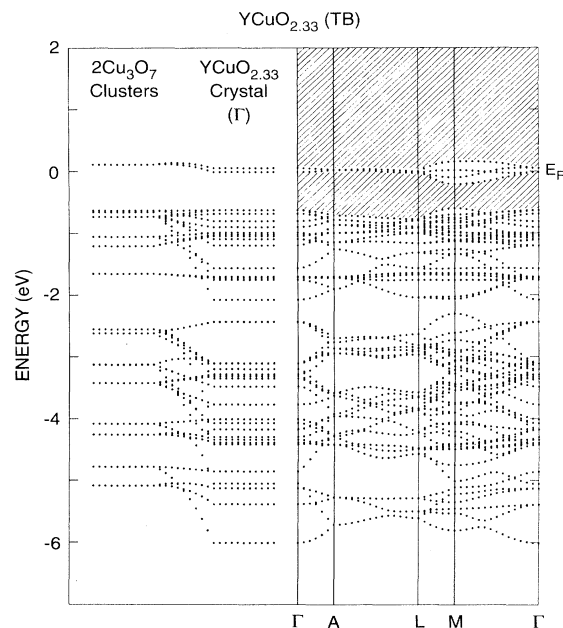


FIG. 3. Evolution of TB Cu_3O_7 cluster levels into $\text{YCuO}_{2.33}$ band states for a hypothetical $H(\sqrt{3}\times\sqrt{3})$ phase in which the uppermost cluster level is transformed into narrow impurity bands in the crosshatched YCuO_2 semiconductor gap.

Y(4d) states. Soft x-ray-absorption data⁷ indicate a gap that is somewhat larger (~ 3.0 eV), thus suggesting that the LDA may underestimate the optical gap. The corresponding results for the hypothetical YCuO_3 phase are shown to the right. The two extra O's per cell add six bands and eight electrons to the valence complex and this leads to partially filled bands and metallic behavior. Both systems exhibit three-dimensional (3D) rather than 2D band characteristics.

The nature of the O-induced bands in the $\text{YCuO}_{2+\delta}$ superoxides is clarified by considering initially a hypothetical $\delta = \frac{1}{3}$ compound in which the filled and empty O sites in Fig. 1(c) are interchanged. This truncates the strong planar Cu-O bonds that form the continuous 1D and 2D networks of the $M(\sqrt{3} \times 2)$ and $H(\sqrt{3} \times \sqrt{3})$ superlattices, leaving an array of essentially isolated Cu_3O_7 clusters. These Cu_3O_7 clusters consist of three O-Cu-O sticks [as seen, for example, in the upper part of Fig. 1(a)] which are bonded together by a central O in the Cu plane. The TB results in Fig. 3 trace the evolution of these Cu_3O_7 cluster levels into bulk 3D $\text{YCuO}_{2.33}$ bands as intercluster TB interactions are switched on. The highest half-filled cluster level evolves continuously to form a complex of split-off impurity-type bands in the forbidden gap of undoped YCuO_2 . The remnant bandwidth of this impurity manifold is due to small intercluster O-O and Cu-Cu interactions.

Normally, one would expect the interstitial O levels to fall within the O(2p) bands. In fact, this is the first superoxide system where self-doping is predicted to produce impurity-type states in the host semiconductor gap. Analysis shows that each interstitial O introduces two bands and two electrons into the gap region. For book-keeping purposes, one can regard these as O-derived p_x, p_y impurity levels which are pushed into the gap by planar σ -bonding interactions with neighboring Cu $d_{xy}, d_{x^2-y^2}$ orbitals, leaving the weaker bonding p_z levels buried in the valence-band manifold. In fact, the uppermost Cu_3O_7 cluster level in Fig. 3 has predominant Cu(3d) character, including 43% $d_{3z^2-r^2}$, 15% $d_{xy}, d_{x^2-y^2}$, and only 22% admixture of interstitial O p_x, p_y character. These weights are changed only slightly (i.e., to 43%, 15%, and 18%, respectively, at Γ) in the $\text{YCuO}_{2.33}$ crystal. The predominant Cu(3d) component in these O-induced states is consistent with soft x-ray-absorption data.⁷

The systematic impurity level-to-band evolution of these $\text{YCuO}_{2+\delta}$ superoxides is illustrated by the TB results in Fig. 4 where the bands for three ordered superlattices with intermediate compositions $0 < \delta < 1$ are compared. For $\delta \geq \frac{1}{2}$, the neighboring Cu_3O_7 clusters become corner-linked to form continuous planar Cu-O networks with 1D $M(\sqrt{3} \times 2)$ or 2D $H(\sqrt{3} \times \sqrt{3})$ characteristics. This systematically broadens the relatively narrow $\delta = \frac{1}{3}$ impurity band from its initial 0.37-eV width to 0.75 eV (for $\delta = \frac{1}{2}$) and finally 1.04 eV (for $\delta = \frac{2}{3}$). It is clear that these split-off bands will merge into the valence manifold for $\delta > \frac{2}{3}$, in agreement with the $\delta = 1$ LAPW results in Fig. 2.

An alternate picture of the impurity-band evolution

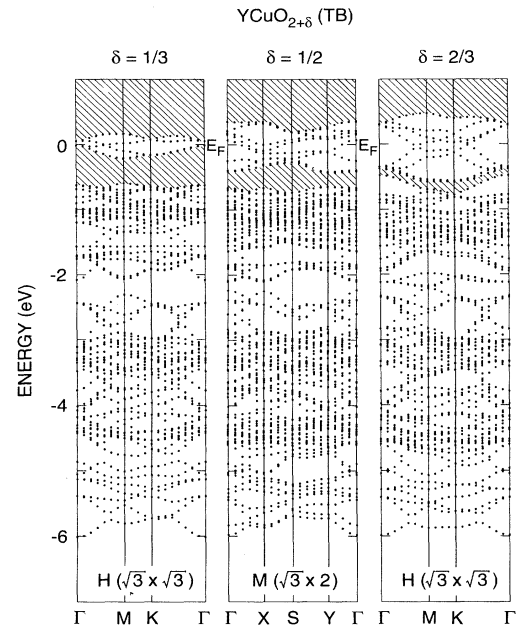


FIG. 4. TB energy-band results for $\text{YCuO}_{2+\delta}$ with $\delta = \frac{1}{3}, \frac{1}{2},$ and $\frac{2}{3}$ which illustrate the impurity level-to-band evolution with increasing δ within the crosshatched YCuO_2 semiconductor gap.

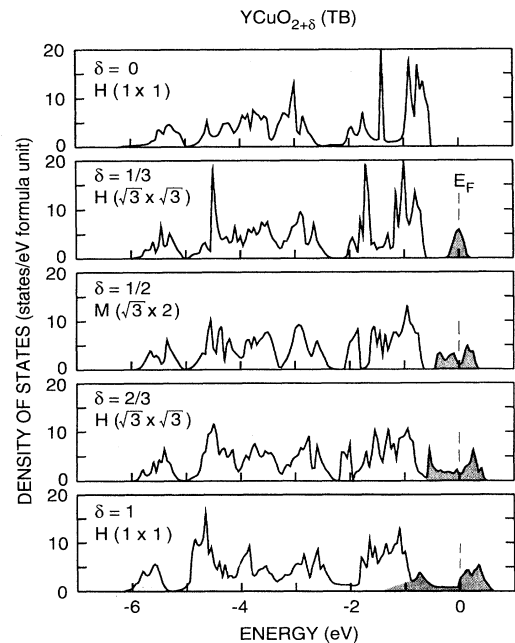


FIG. 5. TB density-of-states results for ordered $\text{YCuO}_{2+\delta}$ phases with $0 \leq \delta \leq 1$. The $\delta = 0$ results have been shifted by -0.5 eV to line up its valence-band features with the corresponding $\delta \neq 0$ results.

with δ is provided by the $\text{YCuO}_{2+\delta}$ density-of-states (DOS) results in Fig. 5. These results show that, in addition to an increasing width, the shaded O-induced impurity bands exhibit significant DOS structure, including a sharp minimum for the $\delta = \frac{1}{2} M(\sqrt{3} \times 2)$ phase. Thus, while normal metallic behavior is predicted for each of these model phases in the absence of antiferromagnetism or structural-relaxation effects, modest changes in the $M(\sqrt{3} \times 2)$ atom-position parameters (which are allowed by monoclinic symmetry) could very well convert the calculated DOS minimum into a gap, thus producing a semiconductor. In fact, transport data⁷ on polycrystalline $\text{YCuO}_{2.51}$ pellets at 300 K suggest semiconducting behavior, with an estimated activation energy of ~ 0.23 eV. Though not shown here, the corresponding Cu(3d) projected DOS results exhibit a δ -dependent feature where the Cu(3d) orbital weight, which is highly concentrated near the top of the valence band (~ 2 eV) at $\delta = 0$, gradually becomes more uniformly distributed for $\delta > 0$. These variations, which are reflected in the LAPW results in Fig. 2, may have important consequences for understanding the magnetic properties of these superoxides.

To summarize, the results of a combined LAPW-TB study of the electronic properties of the delafossite-type $\text{YCuO}_{2+\delta}$ superoxides predict the occurrence of novel, half-filled, O-induced impurity bands in the forbidden gap of undoped YCuO_2 for all compositions $0 < \delta < 1$. Analysis shows that these impurity bands originate from the triangular Cu_3O_7 clusters that represent the basic building blocks of these superoxides. While metallic behavior is predicted for the model O-ordered superstructures that have been considered here, real-world deviations from these idealized structures may open a gap within this impurity band, and thus change the $\delta = \frac{1}{2}$ monoclinic $M(\sqrt{3} \times 2)$ phase from a semimetal to a semiconductor.

I am pleased to acknowledge valuable conversations with R. J. Cava, D. R. Hamann, A. P. Ramirez, and R. E. Walstedt during the course of this investigation. I am especially grateful to I. Natali Sora, Q. Hwang, and A. Santoro at NIST for providing the essence of their $\text{YCuO}_{2+\delta}$ structural results prior to publication.¹¹

¹A. Pabst, *Amer. Miner.* **23**, 175 (1938).

²H. Haas and E. Kordes, *Z. Kristallogr.* **129**, 259 (1969).

³R. D. Shannon, D. B. Rogers, and C. T. Prewitt, *Inorg. Chem.* **10**, 713 (1971); C. T. Prewitt, R. D. Shannon, and D. B. Rogers, *ibid.* **10**, 719 (1971).

⁴S. Okamoto, S. I. Okamoto, and T. Ito, *Acta Crystallogr. Sec. B* **28**, 1774 (1972).

⁵T. Ishiguro, N. Ishizawa, N. Mazutani, and M. Kato, *J. Solid State Chem.* **49**, 232 (1983).

⁶J.-P. Doumerc, A. Ammar, A. Wichainchai, M. Pouchard, and P. Hagenmüller, *J. Phys. Chem. Solids* **48**, 37 (1987).

⁷R. J. Cava, H. W. Zandbergen, A. P. Ramirez, H. Takagi, C. T.

Chen, J. J. Krajewski, W. F. Peck, Jr., J. V. Waszczak, G. Meigs, R. S. Roth, and L. F. Schneemeyer, *J. Solid State Chem.* **104**, 437 (1993).

⁸J. M. Tranquada *et al.*, *Phys. Rev. Lett.* **60**, 156 (1988).

⁹L. F. Mattheiss and D. R. Hamann, *Phys. Rev. B* **33**, 823 (1986).

¹⁰To simplify the superlattice notation in the remaining text, the standard $2H$ designation is suppressed and this basic structure is denoted by $H(1 \times 1)$.

¹¹I. Natali Sora *et al.* (unpublished).

¹²E. Wigner, *Phys. Rev.* **46**, 1002 (1934).